Outer Barrel Stave Mechanical Design Overview for the Proposed CDF SVX Run 2B Detector

Greg Derylo

Fermi National Accelerator Laboratory
Particle Physics Division / Mechanical Department / SiDet
e-mail: derylo@fnal.gov

ABSTRACT

Several design aspects of the proposed Run 2B detector outer barrel stave are considered. The stave's on-board plumbing is investigated to estimate flowrate and heat transfer performance and determine potential plumbing ganging options. The cooling capabilities are then used to estimate stave temperatures to compare predicted silicon temperatures to limit values. Structural stiffness, including both gravitational and differential thermal expansion concerns, is studied to investigate deflections and stresses. A simple accounting of stave radiation length is also included.

The author appreciates the work by Ang Lee (alee@fnal.gov) on the finite element analyses performed for this effort.

1.0 INTRODUCTION

The proposed outer barrel detector is to be constructed in two halves, or barrels, each with four layers of single-sided axial and stereo sensor modules used for tracking between radii of 6.025 and 16.575 cm. An image of a barrel is shown in Figure 1.1. Note that the bulkheads shown do not yet include features that will be necessary for support during barrel assembly, inner detector mounting, outer screen attachment, or structural support within the spacetube. Inner and outer screens are not shown.

A stave (as shown in Figure 1.2), is comprised of three axial and three stereo modules on a cooled core. Stereo sensors can be either small-angle or 90° strips, depending on the layer. Each module consists of two silicon sensors, aligned and glued into a single entity, and a ceramic readout hybrid and pitch adapter that are adhered to the top of one sensor at the outboard end. Axial and stereo sensors have the same length, but slightly different widths to improve SAS coverage. The stave design in shown in greater detail in References 1 and 2.

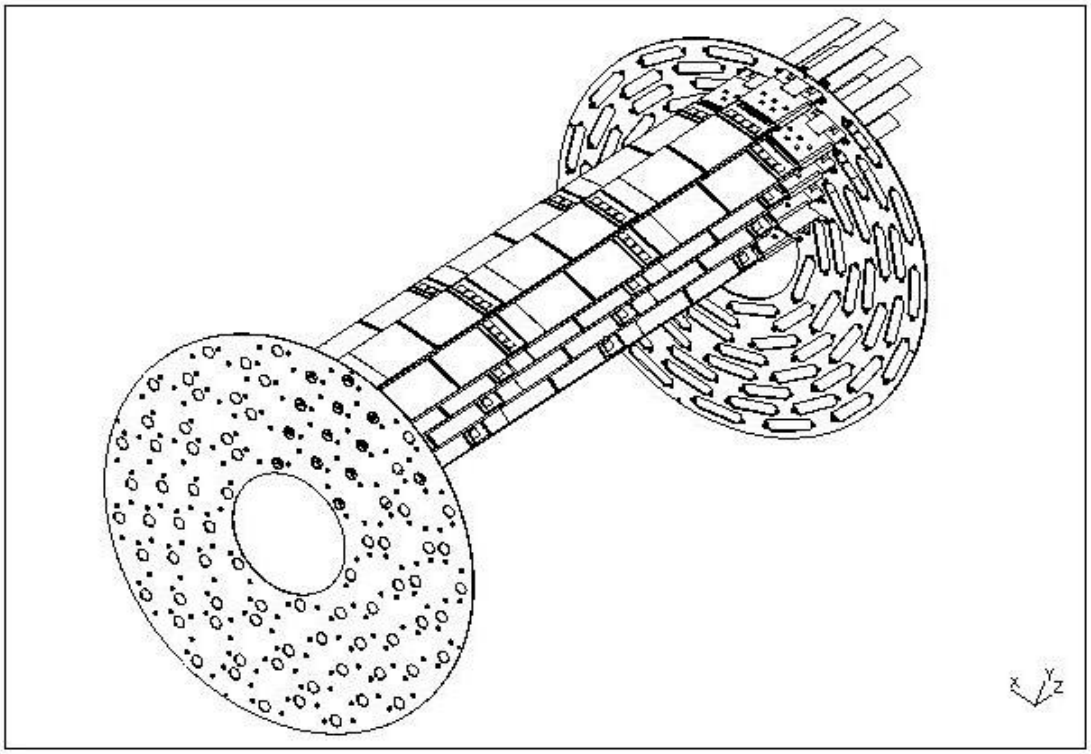

FIGURE 1.1 – Barrel Concept

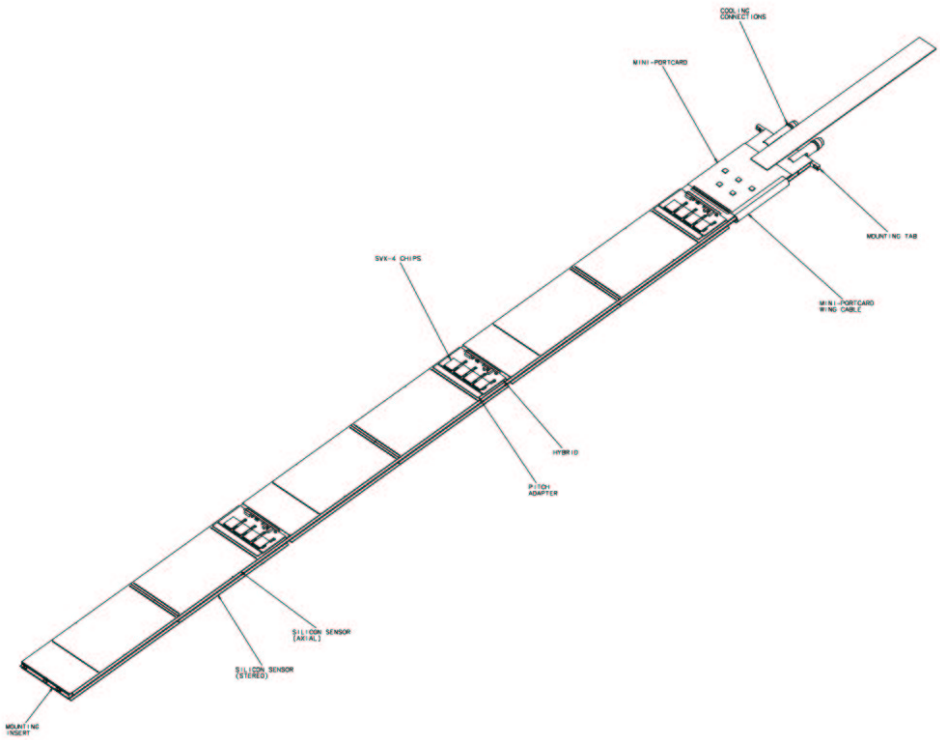

FIGURE 1.2 – Stave Concept

The core consists of two conductive carbon fiber skins laminated over foam and a formed cooling channel. Unlike previous generations of SVX ladders, each ladder will require its own cooling due to the higher luminosity for Run 2B (at least 15 fb^{-1}). The cooling channel is fabricated from thin-walled PEEK tubing, heat-formed into a rectangular cross-section for improved heat transfer. The core also contained mounting hardware at each end for engaging the precision alignment pins on the barrel bulkheads. The mounts on the outer end are slotted to allow alignment during installation. Laminated to the carbon skins are the bus cables, which are ganged together the hybrids on a side of the stave. These cables connect to the three hybrids on each side via wirebonds (a 3 mm gap exists between adjacent modules for this purpose) to the mini-portcard mounted on the end of the stave. The portcard has a flex-cable "wing" that wraps around the edge of the stave and glues to the other side. The bus cable on that side is wirebonded to the wing, thus allowing the mini-PC to handle both sides of the stave. A sample stave cross-section is shown in Figures 1.3 and 1.4.

FIGURE 1.3 – Stave Cross-Section

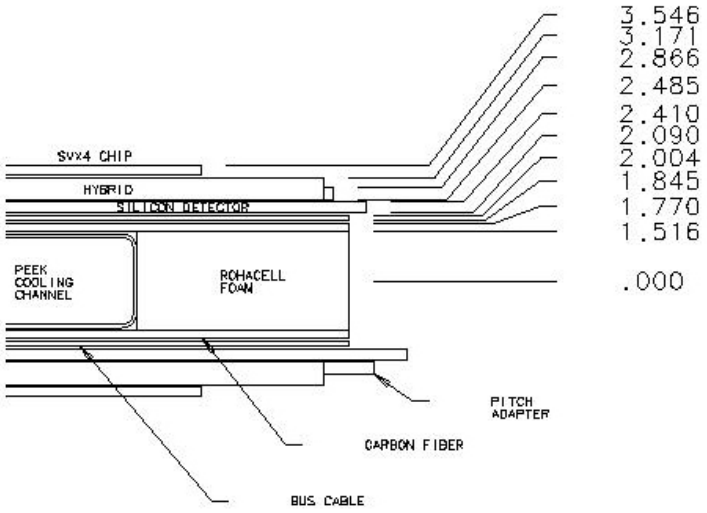

FIGURE 1.4 – Stave Cross-Section Detail

Selected sizes and material properties assumed in mechanical stave studies documented in this report are shown in Table 1.1.

TABLE 1.1 – Material Property Summary

Item	Material	Size (mm)	Density (g/mm^3)	Modulus (GPa)	Conductivity (W/m-K)	CTE (ppm/K)
Sensors	Silicon	T = 0.320 W_A = 40.55 W_S = 43.10 L = 97.012[1]	0.00233	79.92	149	2.6
Hybrid	BeO + Circuit	T = 0.38 W = 38.0 L = 25.0[2]	0.00563 (effective)	345	248	9
Bus Cable	Kapton Assumed (circuit ignored)	T = 0.16 L = 594[3] W = 39.5	0.00148 (effective)	2.5	0.12	20
Carbon Fiber	K13C2U in RS12 Resin [0/90/90/0]	T = 0.25 W = 39.5 L = 652.5[4]	0.00179	Ply Data: E1 = 539 E2 = 5.2 G12 = 3.65	Ply Data: k1 = 372 k2 = 1.5	Ply Data: α1 = 0.27 α2 = 27.5
Foam	Rohacell 51A	T = 3.03	0.000052	0.098	0.029	33
Cooling Tube	PEEK	flat channel width for thermal contact = 4	0.00105	0.49	0.25	46.8
MiniPC	BeO + circuit	T = 0.35 + 0.16 bottom glass W = 39.5 L = 43.18[5]	(as above)	(as above)	(as above)	(as above)
Epoxy	---	0.075 thickness generally assumed	0.00125	3.2	0.1[6]	44

[1] Compares to 96.392 mm for the most recent design.
[2] Compares to 20.0 mm for the most recent design.
[3] Compares to 592 mm for the most recent design.
[4] Compares to 661 mm for the most recent design
[5] Compares to 50.8 mm for the most recent design.
[6] Actual epoxy conductivities are typically about 0.2 W/m-K, but a reduced value was used here for added conservatism.

2.0 PLUMBING ANALYSIS

A preliminary investigation of stave plumbing was investigated in Reference 3. An update to the plumbing study is re-performed here based on updated detector design information. Only the outer barrel staves (currently labeled layers 2 through 5) are considered here. The inner detector design (layers 0 and 1) is not yet understood. The following assumptions are made:

1. Cooling fluid is 42.5% weight ethylene glycol in water at -15°C (the effect of coolant warming along the path is conservatively ignored). Fluid properties are shown in Table 2.1.
2. The tube has an ID, when round, of 0.195" (4.953 mm). Squashed, it has an internal height of 2.68 mm, an internal width of 5.40 mm, and a hydraulic diameter of 3.694 mm. A tube roughness equivalent to that for drawn tubing was assumed.
3. Tube length per stave = 1.26 m plus an additional L/D of 100 for the 180° bend.
4. An additional pressure drop was assumed for a jumper tube when more than one stave were joined in series (0.25 m length with 4.37 mm ID).
5. A laminar friction factor of 64/Re was used for the pressure drop calculation (a wide range of cases investigated yielded no Re valued above 400).
6. Mean Nusselt numbers were estimated for x^* values (dimensionless position in the thermal entry region) based on half of the tube length (complete mixing assumed in 180° horse-shoe turn) using a fit to the data in Reference 4 Table 5.33 on mean Nu in the thermal entrance region of rectangular ducts with constant heat flux boundary conditions. Although Table 5.30 of that reference indicates a benefit for 2 rather than 4 walls convecting heat, no credit was taken for this benefit. Note that x^* is calculated as follows:

$$x^* = (L / D_h) / (Re * Pr)$$

7. The following heat loads are assumed:
   - A. SVX4 Chips: (24 chips) * (0.4 W/chip) = 9.6 W
   - B. Convection: (3 W/m^2-K) * (0.7*0.08 m^2) * (25 K) = 4.2 W
   - C. MiniPC: (5 chips) * (0.5 W/chip) = 2.5 W
   - D. Leakage [5,6]: (6 sensors) * (40 μA/cm^2 at 30 fb^{-1} and R = 6 cm) * (9.64*4.3 cm^2/sensor) * (0.65 at +15°C) * (250 V) = 1.6 W
   - E. The resulting total is 17.9 W per stave. A value of 20 W is assumed for conservatism.

TABLE 2.1 – Fluid Properties of 42.5 wt.% Ethylene Glycol in Water [7]

Temperature (°C)	ρ **(kg / m^3)**	**c_p (J / kg K)**	**k (W / m K)**	μ **(cp)**
-20	1071.98	3334	0.371	15.75
-15	1070.87	3351	0.377	11.74
-10	1069.63	3367	0.383	9.06
-5	1068.28	3384	0.389	7.18
0	1066.80	3401	0.395	5.83
5	1065.21	3418	0.400	4.82
10	1063.49	3435	0.405	4.04
15	1061.65	3451	0.410	3.44
20	1059.68	3468	0.415	2.96

The EES computer code [8] was used to evaluate ΔT, ΔP, and h_{mean} vs. a range of flowrate values for one, two, and three staves plumbed in series, as shown in Figures 2.1 through 2.4. Operation is series helps minimize the total number of inlets/outlets needed, thus simplifying the system. Figure 2.3 is especially helpful in evaluating the

potential for daisy-chaining. With an available pressure drop of about 4.5 psi, the resulting flowrate, ΔT, and h_{mean} are shown in Table 2.2. It is, of course, recommended that testing be performed to verify actual performance as actual stave prototypes become available.

TABLE 2.2 – Plumbing Estimates for 1, 2, and 3 Staves in Series with ΔP = 4.5 psi

	1 Stave	2 Staves	3 Staves
Flowrate (lpm):	0.755	0.358	0.234
$T_{out} - T_{in}$ (°C):	0.44	1.87	4.28
Velocity (m/s):	0.89	0.44	0.30
Re:	302	154	113
x^*:	0.005	0.011	0.016
Nu_{mean}:	10.3	8.3	7.4
h_{mean} (W/m^2-K)	1044	839	730

Previous investigations of ladder chaining had found two ladders in series to be the most reasonable plumbing configuration. These new results indicate that it may be possible to operate the detector with three ladders in series, further simplifying the system. This difference is driven by the larger and taller tube size than previously assumed (0.175" round ID, squashed to an inside height of 0.066" [3]).

With five inlet/outlet slots through the CDF 30° End Plug region available per end for SVX plumbing, the breakdown of heat loads and flowrates with possible slot arrangements, assuming a layer-by-layer ganging scheme, is shown in the following Table. Due to the different ladder count on each layer, this approach results in a large flowrate difference between different slots. The ability of the cooling system to deliver the maximum slot flowrate values should be verified.

TABLE 2.3 – Plumbing Summary of Heat Loads, Flowrates, and System Configuration Assuming Sets of 3 Staves are Connected in Series (Layer-by-Layer ganging)

Slot	Layer	Heat Load per End (W)	No. of Supply & Return Sets per End	Flowrate per End (lpm)	Slot Manifolding Needed per End	Nominal Slot DT (°C)
1	0 & 1	TBD	TBD	TBD	TBD	TBD
2	2	12*20 = 240	12/3 = 4	4*0.24 = 0.96	1-to-4	4.3
3	3	18*20 = 360	18/3 = 6	6*0.24 = 1.44	1-to-6	''
4	4	24*20 = 480	24/3 = 8	8*0.24 = 1.92	1-to-8	''
5	5	30*20 = 600	30/3 = 10	10*0.24 = 2.40	1-to-10	''
Predicted Run 2B Totals	---	1680 + Layers 0&1	28 + Layers 0&1	6.72 + Layers 0&1	---	---
Predicted Run 2A Totals [9]	---	1320 + L00	---	12870 g/min (12.28 lpm) plus L00	---	1.5°C BHs 2.0°C PCs
Actual Run 2A Totals [10]	3 BH slots 1 PC slot 1 L00 slot	---	---	BHs = 8.8 PCs = 3.4 L00 = 2.8	BHs 1-to-5 PCs 1-to-6 L00 = mess	---

A more symmetric scheme can be devised by grouping the Outer Barrel staves into equal groupings, as shown in Figure 2.5. The resulting flowrate and heat load summary is shown in Table 2.4. A more thorough consideration of supply/return tubing configuration, manifold design, ease of testing during barrel assembly, system capabilities, etc. will have to be made to fairly compare these options.

TABLE 2.4 – Plumbing Summary of Heat Loads, Flowrates, and System Configuration Assuming Sets of 3 Staves are Connected in Series (Equal O.B. Stave Count Ganging)

Slot	Layer	Heat Load per End (W)	No. of Supply & Return Sets per End	Flowrate per End (lpm)	Slot Manifolding Needed per End	Nominal Slot DT (°C)
1	0 & 1	TBD	TBD	TBD	TBD	TBD
2	See Fig. 2.5	21*20 = 420	21/3 = 7	21*0.24 = 1.68	1-to-7	4.3
3	‘’	‘’	‘’	‘’	‘’	‘’
4	‘’	‘’	‘’	‘’	‘’	‘’
5	‘’	‘’	‘’	‘’	‘’	‘’
Predicted Run 2B Totals	---	1680 + Layers 0&1	28 + Layers 0&1	6.72 + Layers 0&1	---	---
Predicted Run 2A Totals [9]	---	1320 + L00	---	12870 g/min (12.28 lpm) plus L00	---	1.5°C BHs 2.0°C PCs
Actual Run 2A Totals [10]	3 BH slots 1 PC slot 1 L00 slot	---	---	BHs = 8.8 PCs = 3.4 L00 = 2.8	BHs 1-to-5 PCs 1-to-6 L00 = mess	---

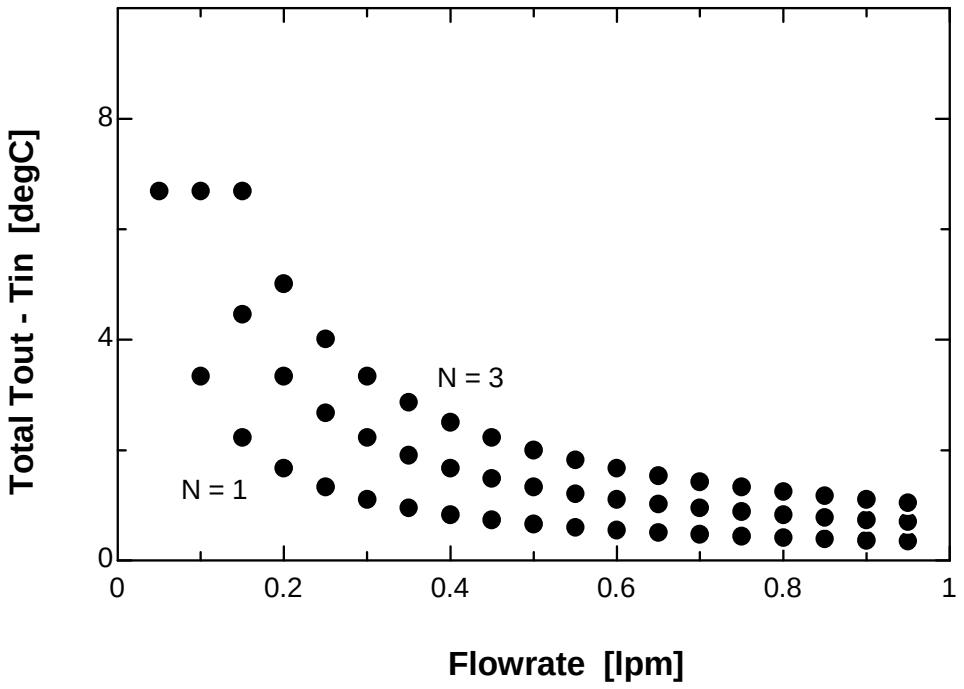

FIGURE 2.1 – ΔT vs. Flowrate for 1, 2, and 3 Staves in Series

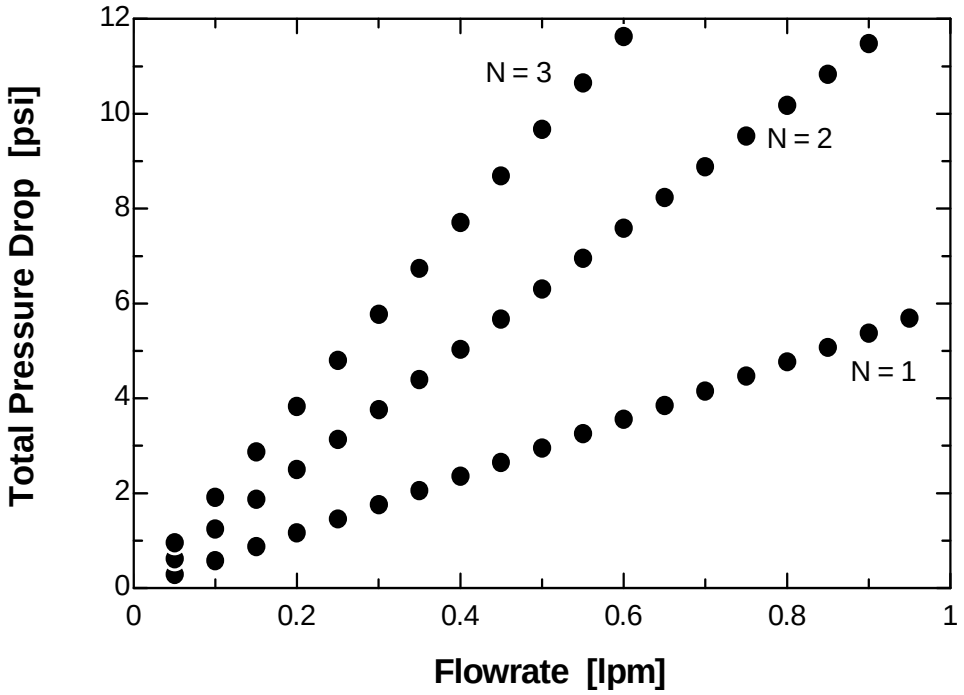

FIGURE 2.2 – ΔP vs. Flowrate for 1, 2, and 3 Staves in Series

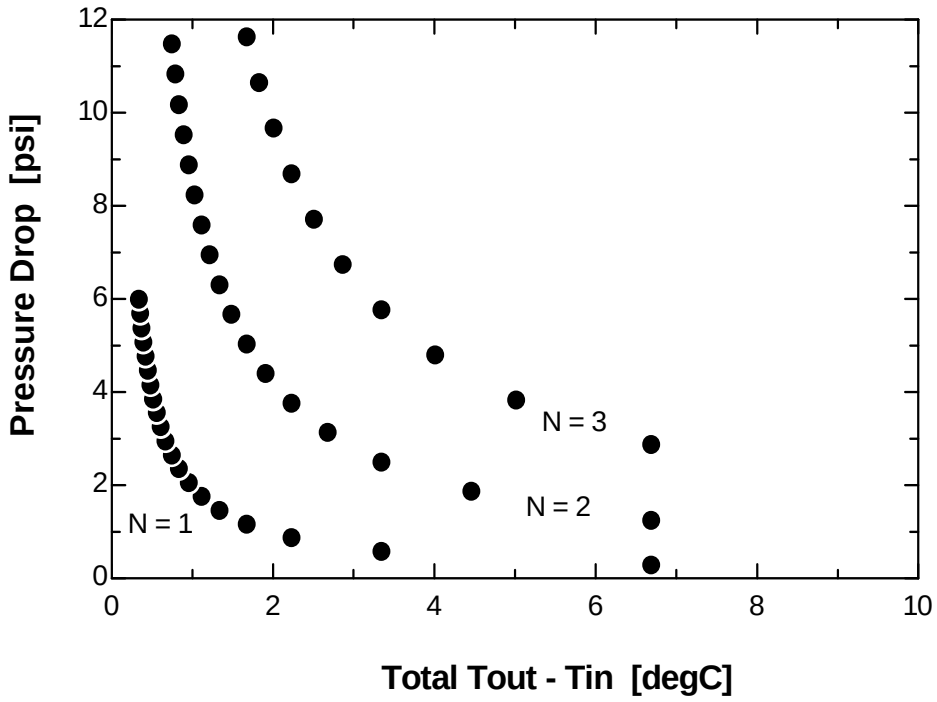

FIGURE 2.3 – ΔP vs. ΔT for 1, 2, and 3 Staves in Series

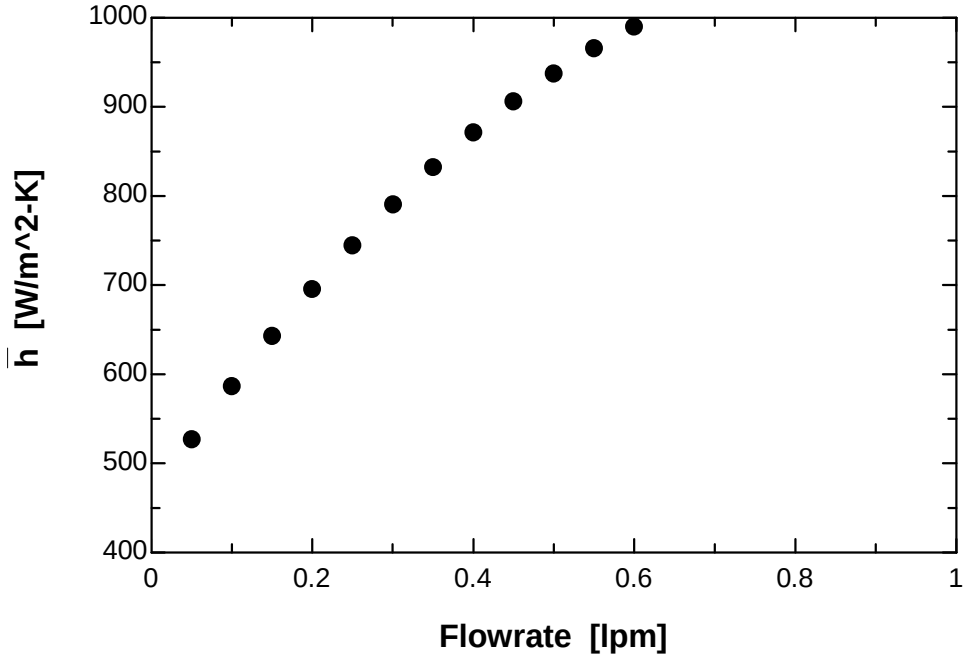

FIGURE 2.4 – Mean Heat Transfer Coefficient vs. Flowrate for 1, 2, and 3 Staves in Series

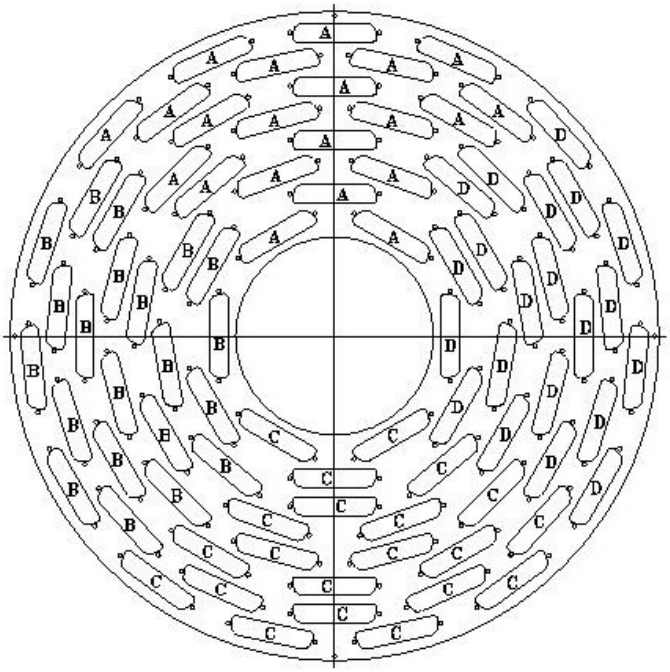

FIGURE 2.5 – Proposed Ganging for Equal Loading of Four Plumbing Slots

3.0 COOLING ANALYSIS

A maximum allowable temperature specification was established by Nicolla Bachetta for the layers present at different radii. For the outer barrel, the temperature limits are:

Layer	Maximum Allowable Average Temperature Along a Module Strip [11,12]
2	+10°C
3	+10°C
4	+15°C
5	+15°C

The outer barrel staves are expected to have considerable margins to these limits since the coolant temperature is driven not by outer barrel performance but by the colder limits placed on Layers 0 and 1, which share the same plumbing system.

A finite element model of the stave was developed by Ang Lee of PPD/MD's Engineering Analysis group to investigate the thermal performance of the stave based on the following assumptions:

a. Heat generation rate = 0.4 W per SVX4 chip

b. Sensor internal heat generation = 0.33 W per sensor (50 $\mu A/cm^2$, +15°C, 250 V). This heat is assumed to be generated uniformly throughout the sensor volume, which may not be the most accurate way to model this complex phenomenon but which is in the end considered to be conservative due to the very high temperature at which this heat load is estimated.

c. Mini-PC transceiver chip heat load = 5 chips * 0.5 W each

d. Convection with -15°C coolant in cooling channel with h = 700 W/m^2-K. With ganging of stave plumbing, the last stave in a series will have an inlet temperature a few degrees warmer. As discussed in Section 2 above, the proposed exit temperature of the last stave is colder than -10°C.

e. Convection with 0°C ambient environment with natural convection h = 3 W/m^2-K

The temperature response for this base case is shown in Figures 3.1 through 3.3. Note that the model makes use of a plane of symmetry down the middle of the ladder to simplify computation. The hottest **axial silicon** temperatures are found underneath the last axial hybrid, where the heat-spreading capabilities of the core skin are limited due to the presence of the nearby mini-PC and its large heat load. For the hottest axial module, a maximum average temperature along a strip was estimated to be about **–10°C** based on the results shown in Figure 3.2.

For a **90° stereo** module, the maximum average temperature along a strip is higher since, at the warmest point, it runs almost entirely underneath the hybrid. However, four ghosted strips in a module are ganged together on a single chip readout channel, so the average temperature of all four strips is the value of concern [12]. Even assuming the warmest individual strip is at about -4°C, the other strips, being cooled to much lower temperatures, results in a maximum average value colder than approximately **–9°C** for the case represented in Figure 3.2.

For a stave with a **small-angle stereo** sensor instead of a 90° sensor, the majority of the strips would be colder than its axial counterparts since they are similar to the axials in that they are only partially covered by hybrids but they do not have a miniPC mounted on their side of the stave. However, some strips are considerably shorter that the full module length, with the shortest ones being entirely within the hybrid region. For the results represented by Figure 3.2, the maximum average strip temperature would be less than **–4°C**.

Additional cases were run to investigate the sensitivity of maximum sensor temperature to various parameters. The results of several of these cases are listed below:

Convection Coefficient (W/m^2-K)	**Single Ply Carbon Fiber Conductivity (W/m-K)**	**Maximum Sensor (not max. avg.) Temperature (°C)**
700	k1 = 372 / k2 = 1.5	-2.9 (Figure 3.2 Results)
800	k1 = 372 / k2 = 1.5	-3.3
800	k1 = 125 / k2 = 0.5	-2.1

Based on these results, it appears that significant margin exists between the estimated temperatures and the specification. Again, the colder requirements for the inner detectors requires that the outer barrel staves be operated colder than necessary due to the shared plumbing system.

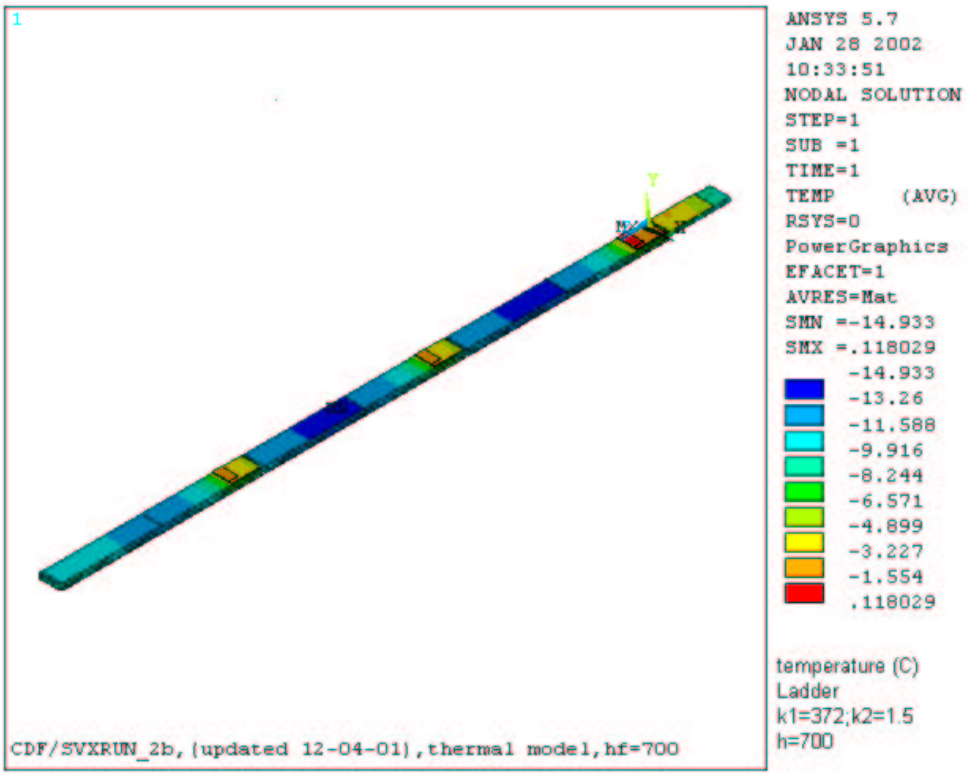

FIGURE 3.1 – Overall Temperature Profile

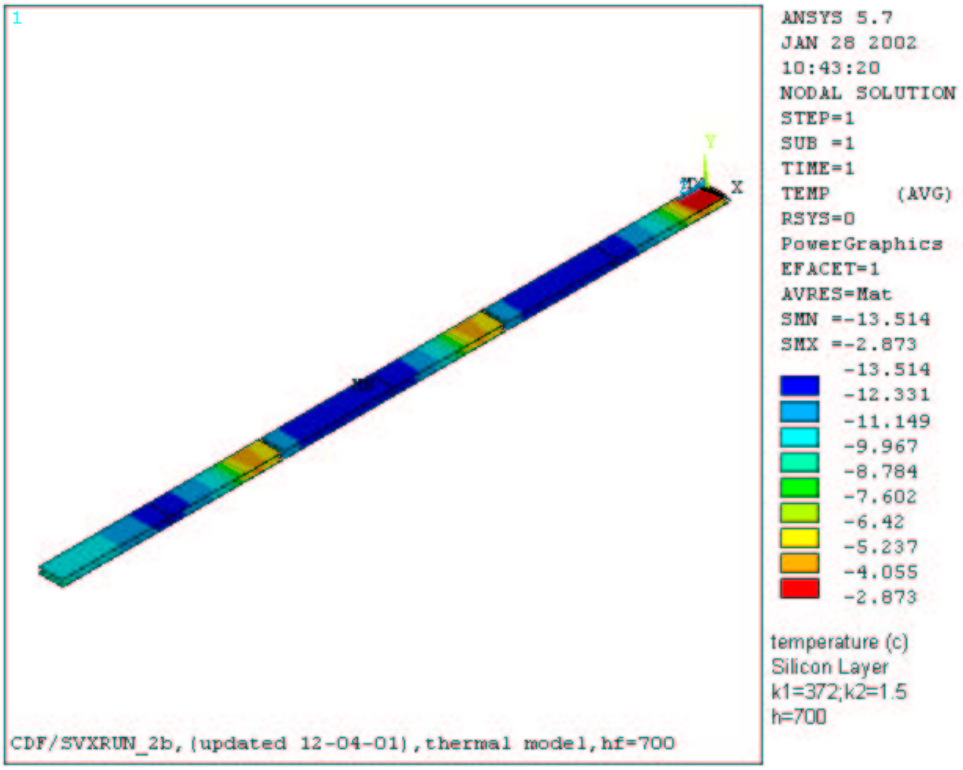

FIGURE 3.2 – Silicon Temperature Profile

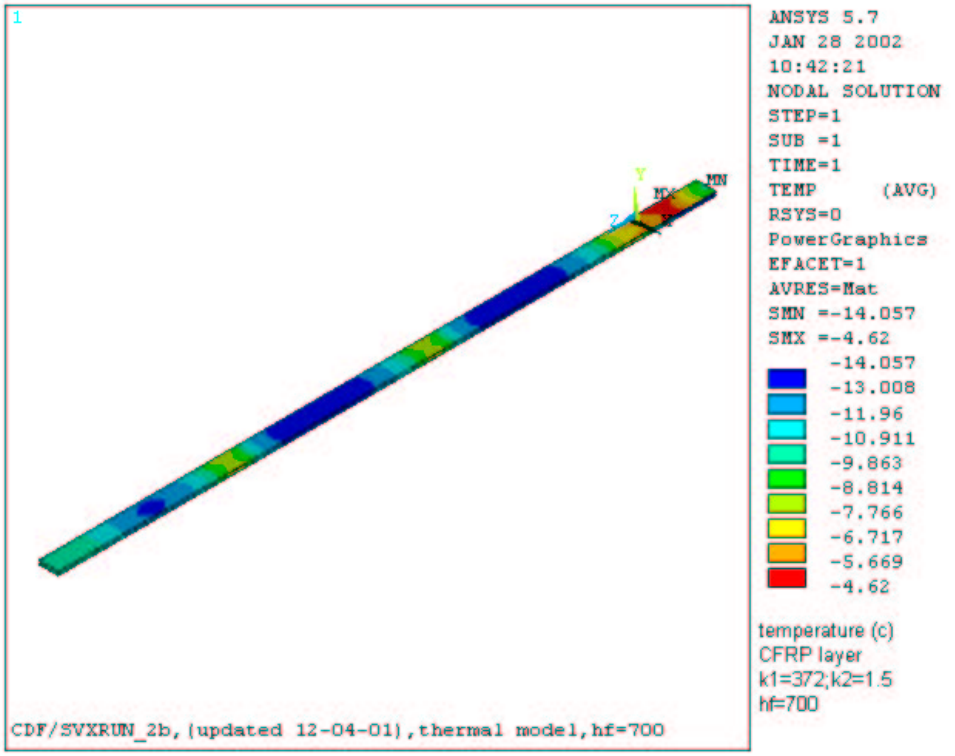

FIGURE 3.3 – Carbon Fiber Temperature Profile

4.0 STRUCTURAL ANALYSIS

4.1 Nominal Deflection Study

The FEA model was used to investigate ladder stiffness. Due to the long, thin nature of the stave's design, gravitational bowing was one of the early design concerns. Figure 4.1.1 shows the effect of gravity on a horizontal ladder with "free" boundary conditions on each end. The maximum sag found was 149 μm. With a fixed-slope boundary condition at the outer end of the ladder, the sag is slightly reduced (to 133 μm), as shown in Figure 4.1.2.

Ladder deformations and their effect on misalignment has been under consideration [13]. Alignment specifications at this time are still considered to be preliminary.

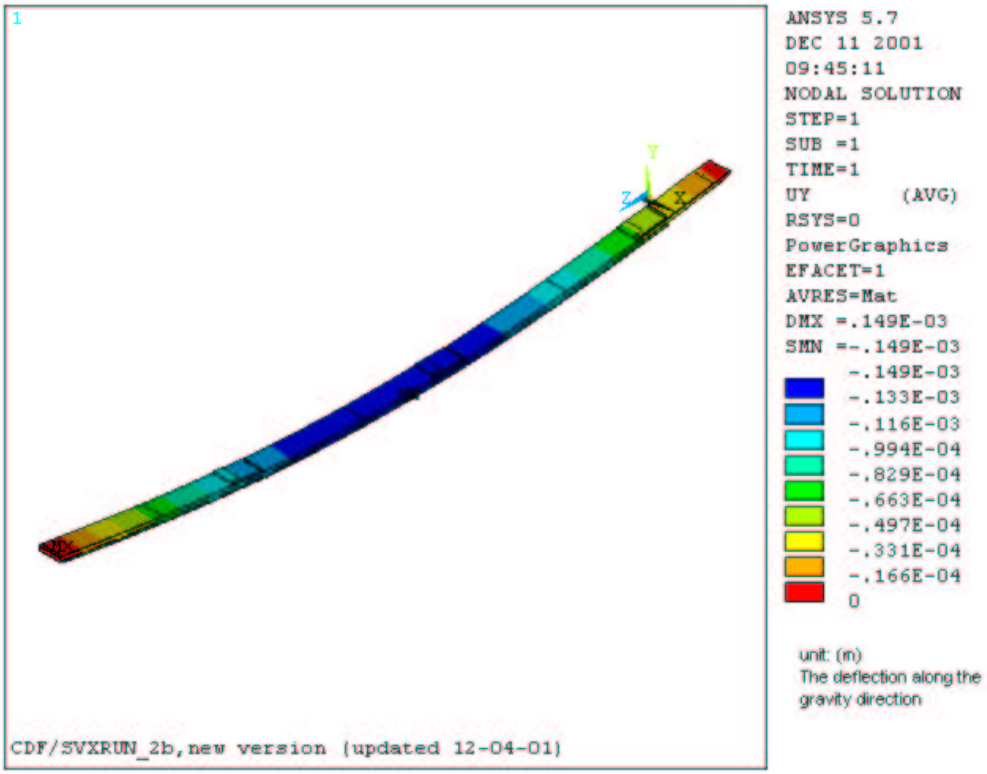

FIGURE 4.1.1 – Gravitational Sag with Free Slopes on Ends
[Max Sag = 149 μm]

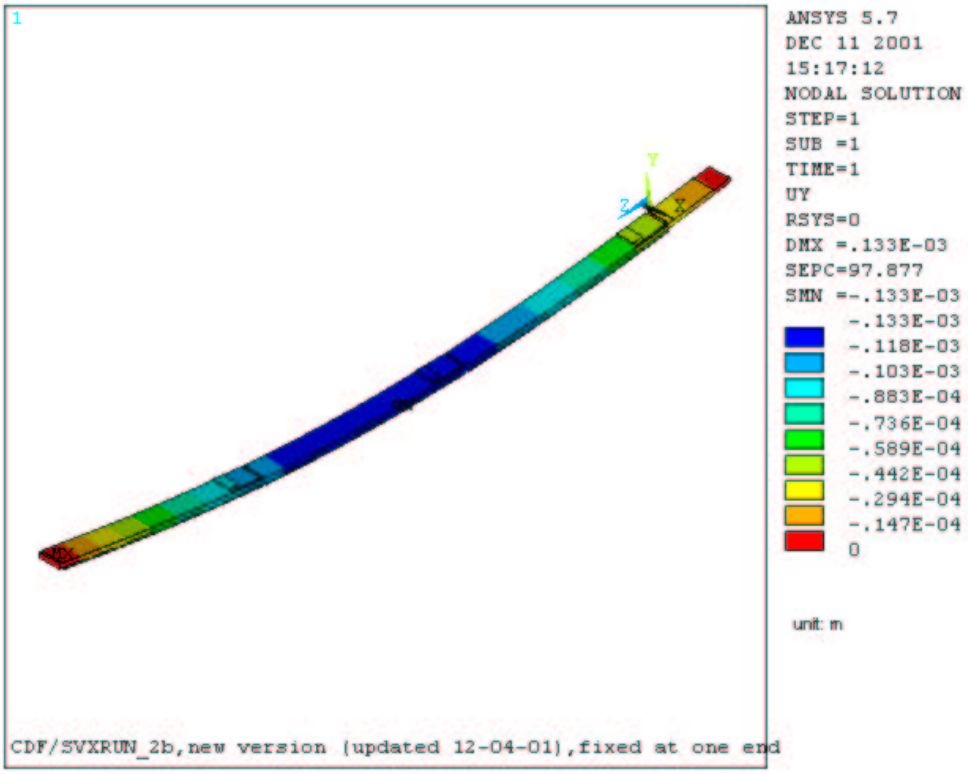

FIGURE 4.1.2 – Gravitational Sag with Free Slope on Inner End And a Fixed Slope on the Outer End [Max Sag = 133 μm]

4.2 Cooldown from +20°C to -15°C

Additional FEA cases were investigated to study the effect of differential thermal expansion during a cooldown from ambient condition (+20°C) to a cooled but unpowered condition (uniform temperature of -15°C assumed). The effect of gravity for a horizontal ladder is also included in this study. Figures 4.2.1 through 4.2.3 show the deflections in the ladder and show a maximum value of 205 μm, which is 56 μm worse that that found above for the deflection study performed without this thermal effect. Although the stave design is largely very symmetric, which minimizes thermal deflection effect, the stave region in the area of the miniPC does not maintain this symmetry. This effect contributes to the added deflection.

Figures 4.2.4 though 4.2.6 show the stresses calculated in the silicon, glue, and carbon fiber skins. These results, as well as the stresses reported in the foam and PEEK [14], are summarized in the table below:

Material	Figure	Calculated Maximum Stress (ksi)	Limit Stress (ksi)
Silicon	4.2.4	4.3	17.4 (yield)
Epoxy	4.2.5	2.2	~ 2 or 3 (shear st.)
Carbon Fiber Skins	4.2.6	18.5	> 100 (tensile st.)
Rohacell 51	---	0.1	0.27 (tensile st.)
PEEK	---	1.5	18 (tensile st.)

For the silicon, the maximum stress was found at the detector corner underneath a hybrid, which is where the CTE differences are most severe. For the epoxy, the maximum is found at a corner in the epoxy between the hybrid and the Si. This edge effect is very localized – the stresses are maintained below 1 ksi for the vast majority of the stave.

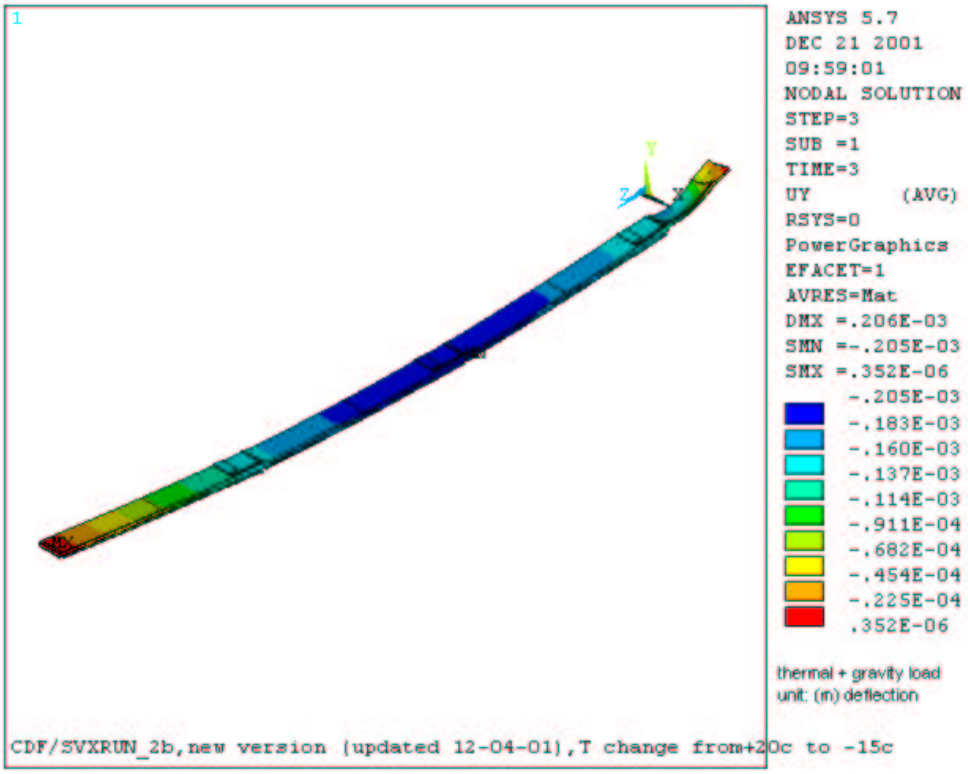

FIGURE 4.2.1 – Deformations from Cooldown from +20 to -15°C Plus Gravitational Sag [Max Sag = 205 μm]

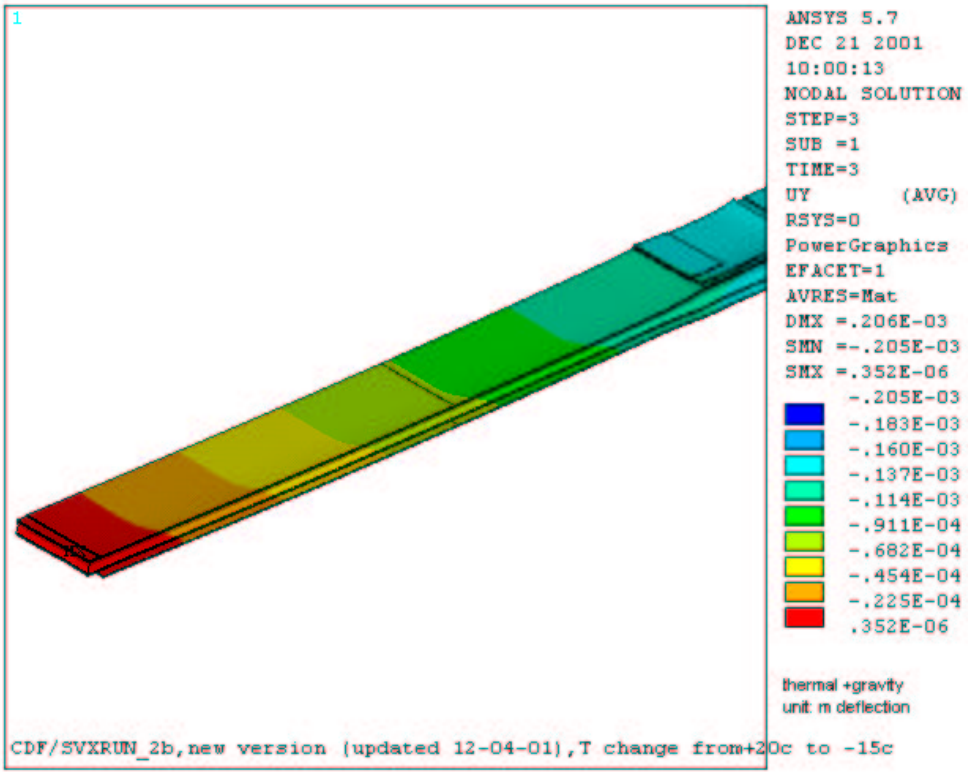

FIGURE 4.2.2 – Deformations from Cooldown from +20 to -15°C Plus Gravitational Sag [Zoomed Image]

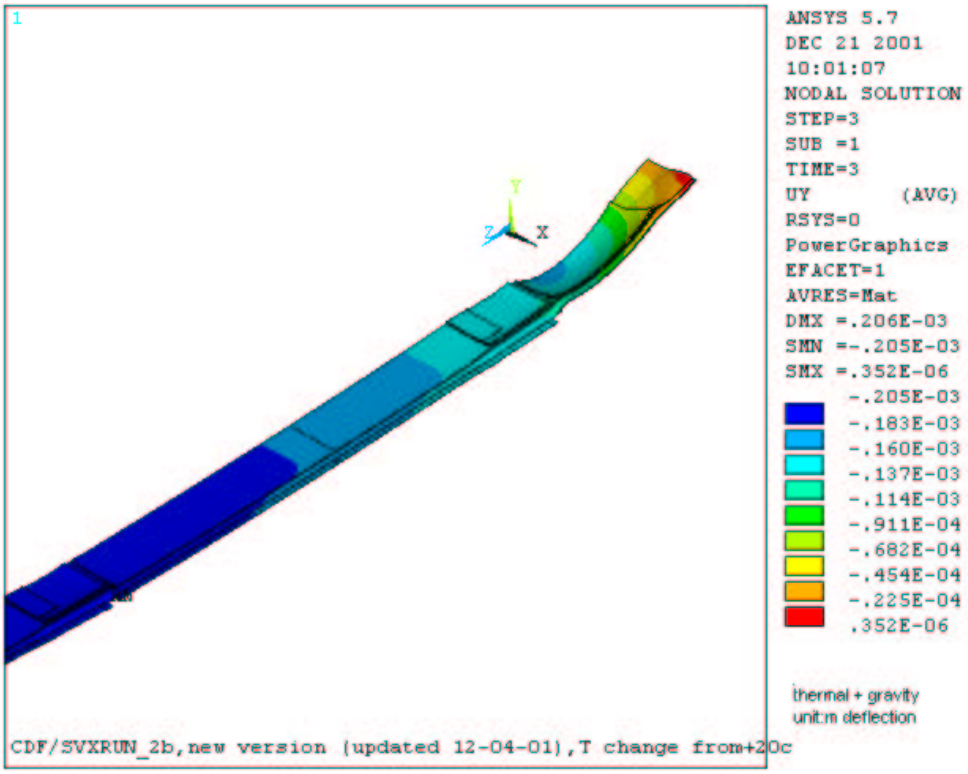

FIGURE 4.2.3 – Deformations from Cooldown from +20 to -15°C Plus Gravitational Sag [Zoomed Image]

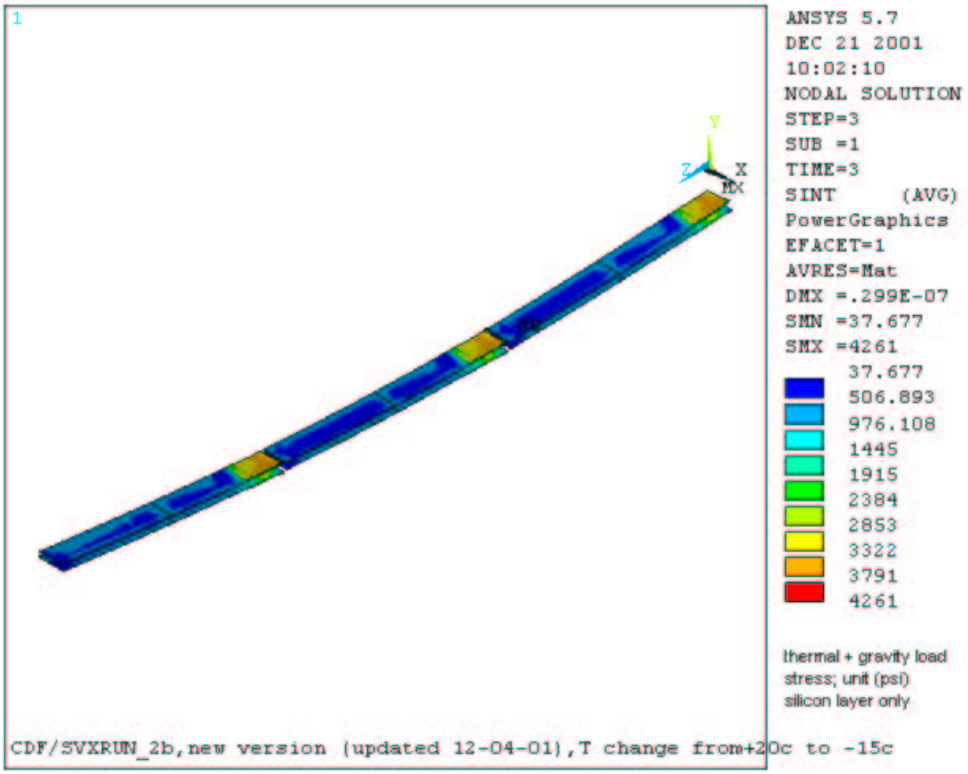

FIGURE 4.2.4 – Silicon Stresses from Cooldown from +20 to -15°C Plus Gravitational Sag

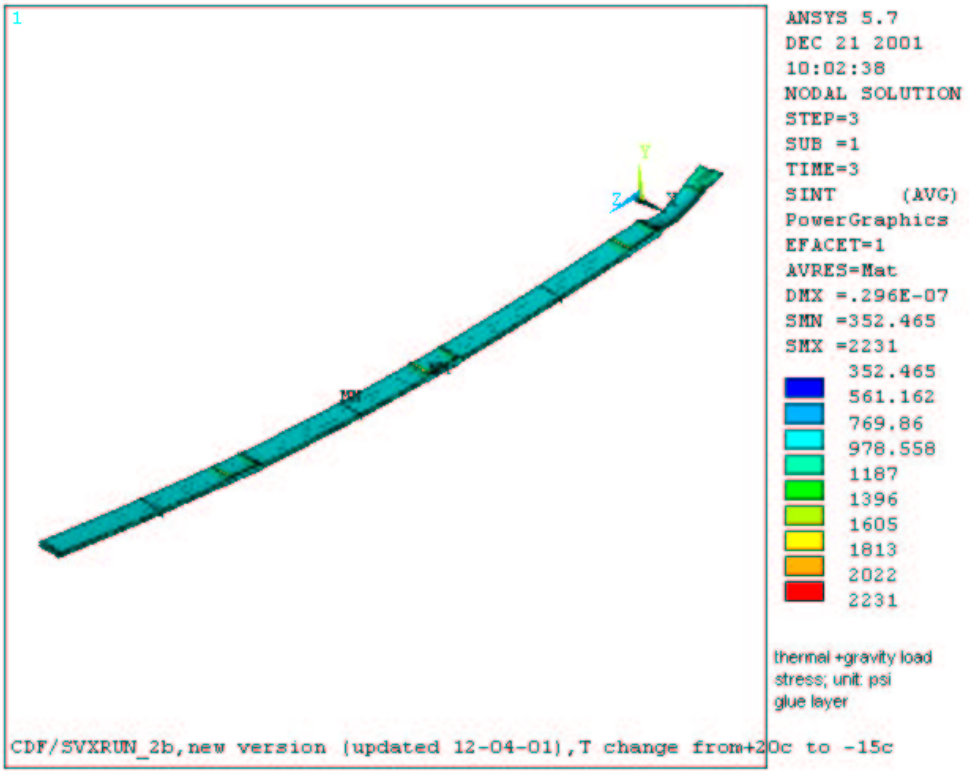

FIGURE 4.2.5 – Glue Stresses from Cooldown from +20 to -15°C Plus Gravitational Sag

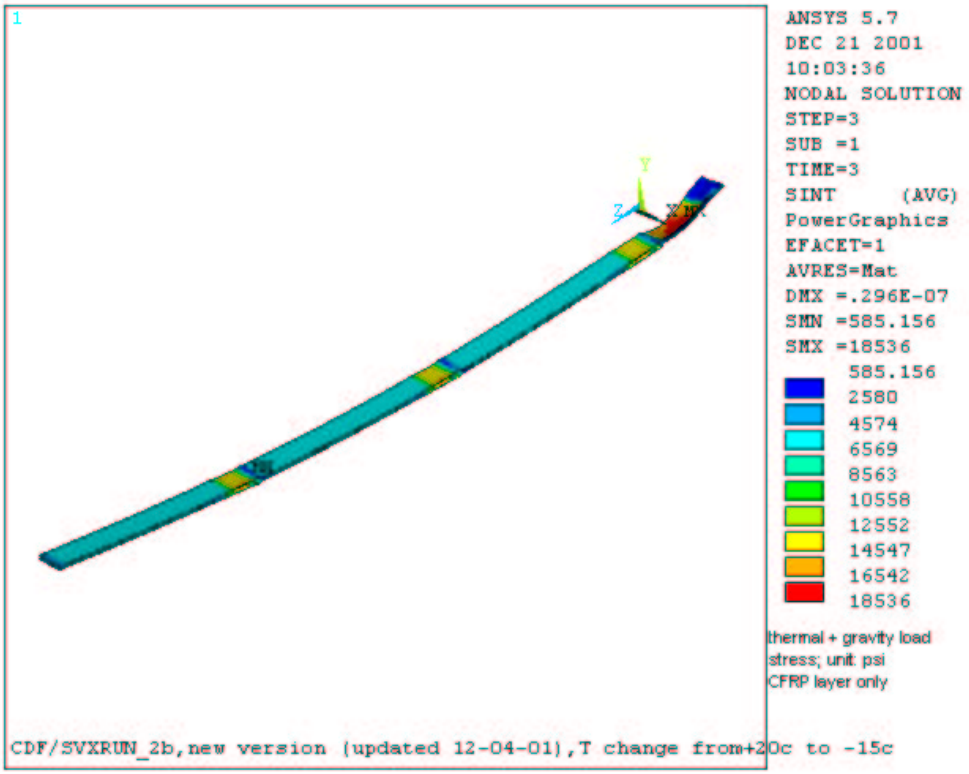

FIGURE 4.2.6 – Carbon Fiber Skin Stresses from Cooldown from +20 to -15°C Plus Gravitational Sag

4.3 Cooldown from +20°C to Operating Conditions

Stresses were also investigated assuming a temperature change from +20°C down to cooled operating conditions to determine if the local temperature gradients resulted in worse stress values than the uniform -15°C case. It was found that warm-up from -15°C to the operating temperature profile reduced the maximum stress values rather than increasing them. The cooldown from room temperature to -15°C are therefore more limiting.

5.0 RADIATION LENGTH ESTIMATE

An attempt has been made to quantify the amount of material in an outer barrel stave from a radiation length standpoint, as shown in the spreadsheet table below. This calculation looks at the material within a stave in the readout area only – material out past the end of the last silicon sensor is ignored.

Detailed estimates in 'phi' and 'eta' have not been performed. Rather, this estimate simply looks at all the material in a single stave in the tracking volume and assumes that it is evenly spread out over the average silicon footprint area (236.83 cm^2) and that the particle path is normal to the surface. Since some of the material is rather clumpy (such as the hybrids, bus cable copper, coolant, and stave mounting block) and particle path directions are widely varied and can pass through overlapping ladders in a single layer, this averaging technique is admittedly simplistic. A more advanced model of detector mass could be compiled as the overall design becomes more complete and as resources allow.

Run 2B Outer Barrel Stave Radiation Length

Mass Averaged over Effective Area of 236.83 cm^2

		Volume Fract.	Length (mm)	Width (mm)	Thickness (mm)	SubAssy Volume (mm^3)	Qty	Total Volume (mm^3)	Density (g/mm^3)	Mass (g)	Matl Rad Length (g/cm^2)	%RL	Percent of Total %RL
Sensors										**39.3**		**0.72**	**39.3**
Axial		1.00	96.39	37.91	0.320	1169.9	6	7016.1	0.00233	16.348	21.82	0.32	17.2
Stereo		1.00	96.39	43.10	0.320	1329.9	6	7976.6	0.00233	18.586	21.82	0.36	19.5
Epoxy	(Si to bus cable)	1.00	96.39	39.50	0.075	285.6	12	3426.7	0.00125	4.283	30.00	0.05	2.5
Silver	(Si to bus cable)	0.15	2.00	2.00	0.216	0.1	36	4.7	0.01050	0.049	9.17	0.00	0.1
Hybrids										**11.7**		**0.24**	**13.0**
BeO		1.00	20.00	38.00	0.38	288.8	6	1732.8	0.00285	4.938	41.31	0.05	2.7
Glass	(SiO2, 3 layers, 38 um each)	1.00	20.00	38.00	0.11	86.6	6	519.8	0.00222	1.154	27.04	0.02	1.0
Gold	(2 layers, 80% coverage, 7.5 um each)	0.60	20.00	38.00	0.01	3.4	12	41.0	0.01930	0.792	6.45	0.05	2.8
Capacitors	(BaTiO3 assumed)					20.2	6	175.2	0.00608	1.065	11.31	0.04	2.2
Resistors	(Alumina assumed)					3.0	6	17.9	0.00326	0.058	27.96	0.00	0.0
Solder	(63/37 Tin/Lead)					8.6	6	51.3	0.00880	0.451	7.72	0.02	1.3
Silver	(die epoxy)	0.15	9.16	6.50	0.03	0.3	24	6.9	0.01050	0.068	9.17	0.00	0.2
SVX4 Die		1.00	9.16	6.50	0.30	17.9	24	428.7	0.00233	0.999	21.82	0.02	1.0
Pitch Adapter	(mounted on Silicon)	1.00	4.00	41.00	0.38	62.3	6	373.9	0.00397	1.483	27.94	0.02	1.2
Epoxy	(hybrid-to-Si, pitch adapter, & SVX4)					81.2	6	487.4	0.00125	0.609	30.00	0.01	0.3
Wirebonds		1.00	3.00	0.02	0.02	0.0	15000	18.0	0.00270	0.049	12.86	0.00	0.1
Bus Cable										**19.6**		**0.32**	**17.4**
Kapton	(3 layers per cable, 1 mil each)	1.00	585.00	39.50	0.075	1733.1	2	3466.1	0.00140	4.853	38.39	0.05	2.9
Copper	(3/4 mil, 80% full)	0.80	400.00	39.50	0.019	240.2	2	480.3	0.00630	4.467	12.86	0.15	8.0
Aluminum	(1/2 mil, Full width)	1.00	585.00	39.50	0.013	300.4	2	600.8	0.00270	1.622	24.01	0.03	1.5
Interlayer Glue	(3 layers, 1 mil each)	1.00	585.00	39.50	0.075	1733.1	2	3466.1	0.00125	4.333	30.00	0.05	2.5
Epoxy	(Bus cable to core)	1.00	585.00	39.50	0.075	1733.1	2	3466.1	0.00125	4.333	30.00	0.05	2.5
Ladder Core										**51.3**		**0.54**	**29.3**
Skin Carbon	(10 mil CF skin)	0.60	585.00	39.50	0.250	3466.1	2	6932.3	0.00215	14.902	32.70	0.15	8.0
Skin Epoxy		0.40	585.00	39.50	0.250	2310.8	2	4621.5	0.00125	5.777	30.00	0.06	3.3
PEEK Tubing	(0.1 mm wall)	1.00	1100.00	15.88	0.100	1746.7	1	1746.7	0.00132	2.306	31.55	0.02	1.3
Coolant	(92.5% EG in water)	1.00	1100.00	14.37	1.000	15807.0	1	15807.0	0.00105	16.597	37.25	0.19	10.2
Foam	(Rohacell 51A)	1.00	585.00	27.00	3.000	47385.0	1	47385.0	0.00005	2.369	91.36	0.03	1.4
Epoxy		1.00	585.00	39.50	0.150	3466.1	2	6932.3	0.00125	8.665	30.00	0.09	5.0
Inner Mount	(Be)	0.90	39.50	2.77	3.125	307.6	1	307.6	0.00185	0.568	65.19	0.00	0.2
Support Hardware										**1.9**		**0.02**	**1.1**
Z = 0 End Support													
Inner Bulkhead Can	(1 mm thk, area divided by the # of ladders)	0.60	1040.32	1.00	1.000	624.2	1	624.2	0.00215	1.342	32.70	0.01	0.7
Inner Bulkhead Epoxy		0.40	1040.32	1.00	1.000	416.1	1	416.1	0.00125	0.520	30.00	0.01	0.3
Pins	(aluminum)					13.2	2	26.5	0.00270	0.072	24.01	0.00	0.1
Outboard Support													
Hardware past end of sensors not included in this study!													

Total =	1.84	%RL
Total =	124	grams

6.0 REFERENCES

1. FNAL Drawing 2563.530-ME-405211, "CDF SVX Run 2B Outer Barrel Stave Assembly."
2. FNAL Drawing 2563.530-ME-405213, "CDF SVX Run 2B Outer Barrel Stave Core Assembly."
3. MD-Eng/01-005, "CDF SVX Run 2B Ladder Cooling for Layers 1 through 6," Greg Derylo, 25 Sep 2001.
4. W.M. Rohsenow, J.P. Hartnett, and Y.I. Cho, ed., "Handbook of Heat Transfer, 3rd ed.," (New York: McGraw-Hill, 1998).
5. Leakage current predictions by Nicola Bacchetta at the Run 2B workshop on 7 May 2001.
6. Information provided by Nicola Bacchetta and Joe Incandella.
7. 1997 ASHRAE Fundamentals Handbook, pp 20.5 – 20.7.
8. Computer code, "Engineering Equation Solver (EES) Version 6.234," by F-Chart Software.
9. CDF/DOC/Tracking/Public/4473, "Characterization of a SVX II Bulkhead," Steve Blusk et. al., 6 Feb 1998.
10. SVX Flow Monitor logbook data for operation at a –5°C setpoint on 8/13/01.
11. E-mail from Nicolla Bacchetta (bacchetta@fnal.gov) on 24 Aug 2001.
12. Conversation with Nicola Bacchetta and Mike Hrycyk, 8 Feb 2002.
13. Informal Report, "CDF SVX2B Outer Barrel Ladders – Consideration of Potential Ladder Misalignments in 'ϕ' and 'R'," by Greg Derylo, 27 Nov 2001, currently posted on http://www-cdf.fnal.gov/internal/people/links/GregoryDerylo/OB/alignment.pdf.
14. E-mail from Ang Lee (alee@fnal.gov) on 29 Jan 2002.